

Article

New In Situ Catalysts Based on Nitro Functional Pyrazole Derivatives and Copper (II) Salts for Promoting Oxidation of Catechol to *o*-Quinone

Abderrahim Titi ^{1,*}, Kaoutar Zaidi ¹, Abdullah Y. A. Alzahrani ², Mohamed El Kodadi ^{1,3}, El Bekkaye Yousfi ^{1,4}, Anna Moliterni ⁵, Belkheir Hammouti ¹, Rachid Touzani ^{1,*} and Mohamed Abboud ^{6,*}

- ¹ Laboratory of Applied and Environmental Chemistry (LCAE), Faculty of Sciences, University Mohammed Premier, Oujda 60000, Morocco
- ² Department of Chemistry, Faculty of Science and Arts, King Khalid University, Mohail Assir 62529, Saudi Arabia
- ³ Laboratoire d'Innovation en Sciences, Technologie et Education (LISTE), CRMEF, Oujda 60000, Morocco
- ⁴ Higher Institute of Nursing and Health Professions Techniques (ISPITS), Oujda 60000, Morocco
- ⁵ Istituto di Cristallografia, CNR, Via Amendola, 122/0, 70126 Bari, Italy
- ⁶ Catalysis Research Group (CRG), Department of Chemistry, College of Science, King Khalid University, P.O. Box 9004, Abha 61413, Saudi Arabia
- * Correspondence: titi_abderrahim1718@ump.ac.ma (A.T.); r.touzani@ump.ac.ma (R.T.); mabboud@kku.edu.sa (M.A.)

Abstract: Herein, new substituted ligands based on pyrazole (L₁–L₄) were synthesized via a one-step by condensing (1*H*-pyrazole-1-yl) methanol with different primary amine compounds. The present work utilized the catalytic properties of the in situ complexes formed by these ligands with various copper (II) salts viz. Cu(CH₃COO)₂, CuSO₄, CuCl₂, and Cu(NO₃)₂ for the oxidation of catechol to *o*-quinone. The studies showed that the catalytic activities depend on the nature and concentration of the ligand, the nature of the counterion, and the solvent. It was observed that the complex formed by L₂ and Cu(CH₃COO)₂ exhibited good catalytic activity in methanol with V_{max} of 41.67 μmol L⁻¹ min⁻¹ and K_m of 0.02 mol L⁻¹.

Keywords: pyrazole; copper; catalyst; oxidation reaction; catecholase; *o*-quinone



Citation: Titi, A.; Zaidi, K.; Alzahrani, A.Y.A.; El Kodadi, M.; Yousfi, E.B.; Moliterni, A.; Hammouti, B.; Touzani, R.; Abboud, M. New In Situ Catalysts Based on Nitro Functional Pyrazole Derivatives and Copper (II) Salts for Promoting Oxidation of Catechol to *o*-Quinone. *Catalysts* **2023**, *13*, 162. <https://doi.org/10.3390/catal13010162>

Academic Editor: Hiroto Yoshida

Received: 5 December 2022

Revised: 4 January 2023

Accepted: 8 January 2023

Published: 10 January 2023



Copyright: © 2023 by the authors. Licensee MDPI, Basel, Switzerland. This article is an open access article distributed under the terms and conditions of the Creative Commons Attribution (CC BY) license (<https://creativecommons.org/licenses/by/4.0/>).

1. Introduction

Pyrazole-based compounds have gathered tremendous advancement in the last decade [1–10] toward numerous versatile applications in the field of bioinorganic and medical sciences. These compounds have been utilized as precursors in the synthesis of many compounds, including artificial metalloenzymes with important biological activities [11–13]. The pyrazole-based ligands have been employed in a wide range of applications, such as electronics [14], catalysis [15–28], and pharmacology [29]; they also exhibit anticorrosion [30], anticancer, antifungal, antiviral, and antibacterial behavior [31,32]. Additionally, they exhibit cytotoxic activities [33,34] and are used for the extraction of lithium and cesium cations [35,36].

Furthermore, the complexation chemistry of these ligands with transition metal ions shows great potential in catalysis, especially in mimicking enzyme activity [37]. One of the important metal ions is copper, which has the ability to combine with various organic ligands to catalyze diverse biological processes. In this regard, a variety of copper-based complexes are employed to study the oxidation reaction of catechol to quinone [19,32,35]. It is remarkable how these complexes can bind reversibly to oxygen under ambient conditions, thus, aiding the reaction [24–28]. Several studies have explored the catalytic activity of copper-based complexes, either in situ [28,32] or through isolated complexes [15–18,35].

Numerous studies have also investigated the catalytic activity of catechol oxidation using a variety of metal complexes, such as iron, cobalt, manganese-based complexes, etc. [22–24]. However, it has been recently reported that copper-based complexes exhibit excellent catalytic activity toward the oxidation reaction [35].

Thus, the present work aims to study the catalytic activity of in situ-prepared pyrazole-based ligands and copper complexes for the conversion of catechol to *o*-quinone in the presence of atmospheric oxygen (O₂). Four different pyrazole-based ligands (L₁–L₄) were synthesized and characterized using ¹H NMR, ¹³C NMR, elemental analysis (EA (%)), and Fourier transform infrared (FT-IR) spectroscopy (please see supplementary information, Figures S1–S15).

2. Experimental Section

2.1. Materials and Characterization Techniques

Catechol, Cu(NO₃)₂, Cu(CH₃COO)₂, CuSO₄, CuCl₂, and solvents, such as methanol, tetrahydrofuran, acetonitrile, and chloroform, were purchased from Aldrich and used as received without further purification.

All compounds were characterized using the ¹H NMR, ¹³C NMR, and IR spectroscopy techniques. ¹H NMR (400 MHz) and ¹³C NMR (100 MHz) spectra were recorded in CDCl₃ at room temperature (Varian Unity-Plus (400 MHz) spectrometer for NMR, and the elemental analyses were retrieved with the help of 2400 Series II CHNS/O elemental analyzer). Chemical shifts (δ) were recorded in parts-per-million (ppm) using tetramethylsilane (TMS) as the internal standard. FT-IR spectra were recorded on a Shimadzu 8201 PC FT-IR spectrophotometer (ν_{max} in cm⁻¹) supported by pressed KBr pellets. The UV-vis absorbance was recorded on a JENWAY 7315-spectrophotometer, and the experiments concerning the oxidation of catechol to *o*-quinone were carried out at the Higher Institute of Nursing and Health Professions Techniques Laboratory, Oujda.

2.2. Synthesis and Characterization

2.2.1. Preparation of Compounds L₁–L₄

The four pyrazole-based ligands (L₁–L₄) were synthesized via a one-step process by the condensation of primary amines and pyrazole derivatives reported in our previous work [38]. Briefly, (1*H*-pyrazol-1-yl) methanol derivatives (1.1eq.) were added to the solution of one equivalent of a primary amine in 10 mL of acetonitrile at room temperature (RT). The reaction was carried out under continuous stirring for 6 h at 60 °C. As the reaction progressed, the solid product separated from the clear and homogenous mixture of amine and (pyrazolyl-1-yl) methanol derivatives in acetonitrile. Thereafter, the unreacted starting material and solvent were removed from the mixture by the filtration process. Subsequently, the isolated product was washed with acetonitrile and ethyl acetate and dried at reduced pressure to remove all the volatile organic compounds. The synthesized pathway is depicted in Scheme 1.

2.2.2. Characterization

N-((1*H*-pyrazol-1-yl)methyl)-4-nitroaniline L₁: This compound was obtained as a yellow solid, yield 85%, M_P: 118–120 °C, **FT-IR:** (KBr, ν(cm⁻¹)): 3256, 3165, 3114, 3023, 2985, 1722, 1605, 1545, 1384, 1214, 1106, 1020, 766; **¹H NMR** (400 MHz, CDCl₃): δH = 5.58 (d, 2H, CH₂), 6.26 (dd, 1H, CH_{Py}), 6.94 (dd, 1H, CH_{Ar}), 7.48 (dd, 1H, CH_{Py}), 7.87 (dd, 1H, CH_{Py}), 8.03 (dd, 1H, CH_{Ar}), 8.24 (t, 1H, NH); **¹³C NMR** (100 MHz, CDCl₃): δC = 58.3 (CH₂), 106.5 (CH_{Py}), 113.8 (CH_{Ar}), 126.1 (CH_{Ar}), 130.4 (CH_{Py}), 139.7 (CH_{Py}), 138.1 (C_{Ar}), 153.2 (C_{Ar}). **EA(%):** Calcd: (55.04)C; (4.62)H; (25.68)N; Obsd: (55.10)C; (4.57)H; (25.63)N.

N-((3,5-dimethyl-1*H*-pyrazol-1-yl)methyl)-4-nitroaniline L₂: This compound was obtained as a yellow solid, yield: 90%, M_P: 128–130 °C, **FT-IR:** (KBr, ν(cm⁻¹)): 3224, 3316, 3230, 3135, 2993, 2920, 1591, 1580, 1487, 1340, 1246, 1230, 1087, 1048, 750; **¹H NMR** (400 MHz, CDCl₃): δH = 2.07 (s, 3H, CH₃), 2.29 (s, 3H, CH₃), 5.41 (d, 2H, CH₂), 5.81 (s, 1H, CH_{Py}), 6.94 (dd, 1H, CH_{Ar}), 8.03 (dd, 1H, CH_{Ar}), 8.12 (t, 1H, NH); **¹³C NMR**

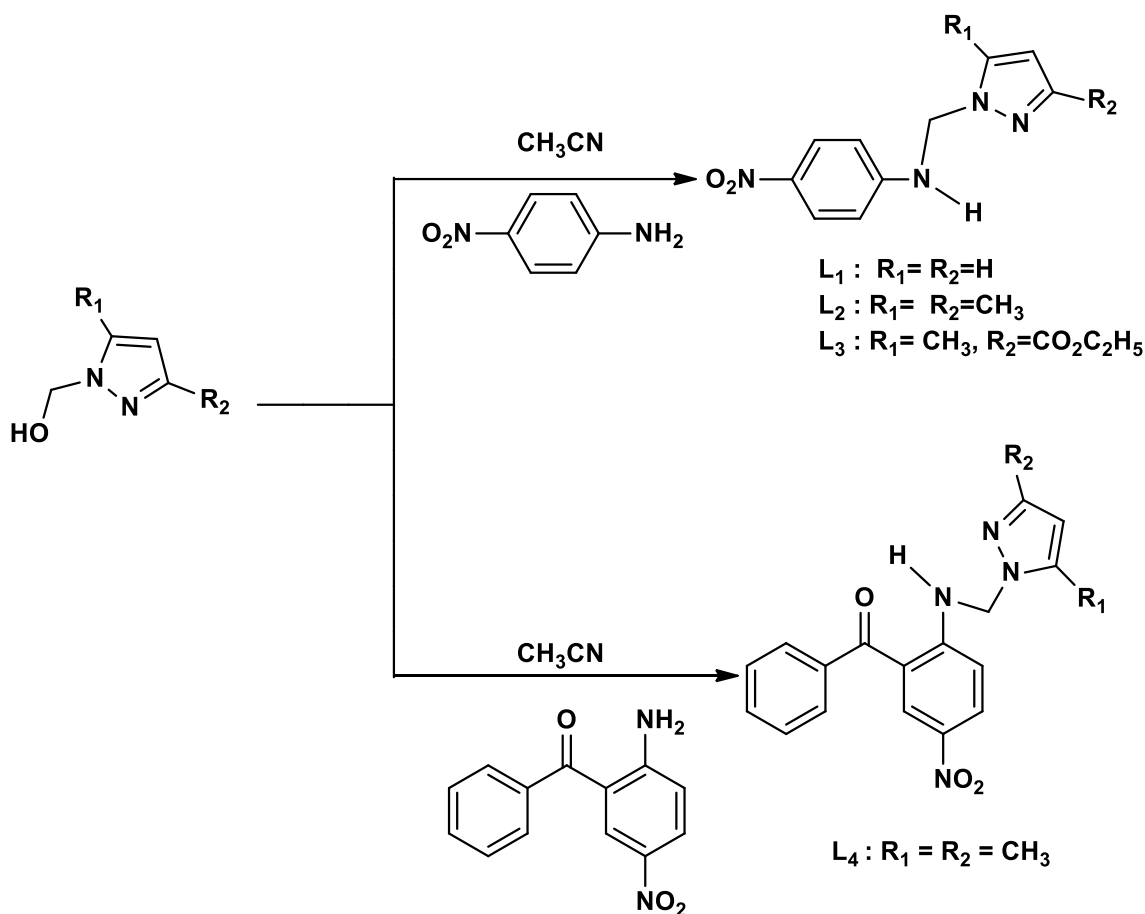
(100 MHz, CDCl_3): $\delta\text{C} = 11.2$ (CH_3), 14.5 (CH_3), 56.7 (CH_2), 106.1 (CH_{Py}), 112.6 (CH_{Ar}), 126.4 (CH_{Ar}), 138.5 (C_{Py}), 139.1 (C_{Ar}), 146.2 (C_{Py}), 153.3 (C_{Ar}). **EA(%)**: Calcd: (58.53)C; (5.73)H; (22.75)N. Obsd: (58.62)C; (5.71)H; (22.65)N.

Ethyl 5-methyl-1-(((4-nitrophenyl)amino)methyl)-1H-pyrazole-3-carboxylate L₃:

This compound was obtained as a yellow solid, yield: 90%, Mp : 125–127 °C, **FT-IR**: (KBr, $\nu(\text{cm}^{-1})$): 3379, 3280, 3129, 2983, 2952, 2836, 1635, 1553, 1456, 1424, 1385, 1310, 1226, 1068, 1040, 805, 765, 702; **¹H NMR** (400 MHz, CDCl_3): $\delta\text{H} = 1.26$ (t, 3H, CH_3), 2.39 (s, 3H, CH_3), 4.24 (q, 2H, CH_2), 5.64 (d, 2H, CH_2), 6.53 (s, 1H, CH_{Py}), 6.95 (dd, H, CH_{Ar}), 8.04 (dd, H, CH_{Ar}), 8.27 (t, H, NH); **¹³C NMR** (100 MHz, CDCl_3): $\delta\text{C} = 11.7$ (CH_3), 15.1(CH_3), 58.4(CH_2), 60.0 (CH_2), 109.4 (CH_{Py}), 112.7 (CH_{Ar}), 126.8 (CH_{Ar}), 138.5 (C_{Py}), 141.2(C_{Ar}), 142.3(C_{Py}), 153.5 (C_{Ar}), 162.6 (CO). **EA(%)**: Calcd: (55.26)C; (5.30)H; (18.41)N. Obsd: (56.01)C; (5.21)H; (18.56)N.

(2-(((3,5-dimethyl-1H-pyrazol-1-yl)methyl)amino)-nitrophenyl)(phenyl)methanone L₄:

This compound was obtained as a yellow solid, yield: 84%, Mp : 94–96 °C, **FT-IR**: (KBr, $\nu(\text{cm}^{-1})$): 3462, 3338, 3264, 3127, 2955, 2847, 1642, 1603, 1479, 1278, 1085, 1055, 766; **¹H NMR** (400 MHz, CDCl_3): $\delta\text{H} = 2.08$ (s, 3H, CH_3), 2.23 (s, 3H, CH_3), 5.22 (d, 2H, CH_2), 5.81 (s, 1H, CH_{Py}), 7.31–8.32 (m, 8H, CH_{Ar}), 8.11 (t, 1H, NH); **¹³C NMR** (100 MHz, CDCl_3): $\delta\text{C} = 11.3$ (CH_3), 14.1 (CH_3), 71.5(CH_2), 106.2 (CH_{Py}), 115.5 (CH_{Ar}), 117.5 (CH_{Ar}), 129.3(CH_{Py}), 129.2 (CH_{Ar}), 129.1 (CH_{Ar}), 129.7 (CH_{Ar}), 130.3(CH_{Ar}), 130.5(CH_{Ar}), 132.3(CH_{Py}), 132.1 (CH_{Ar}), 135.8 (C), 139.1 (C), 139.4 (C), 157.6(C), 197.7 (CO). **EA(%)**: Calcd: (62.75)C; (7.12)H; (30.13)N. Found: (62.81)C; (7.08)H; (30.21)N.

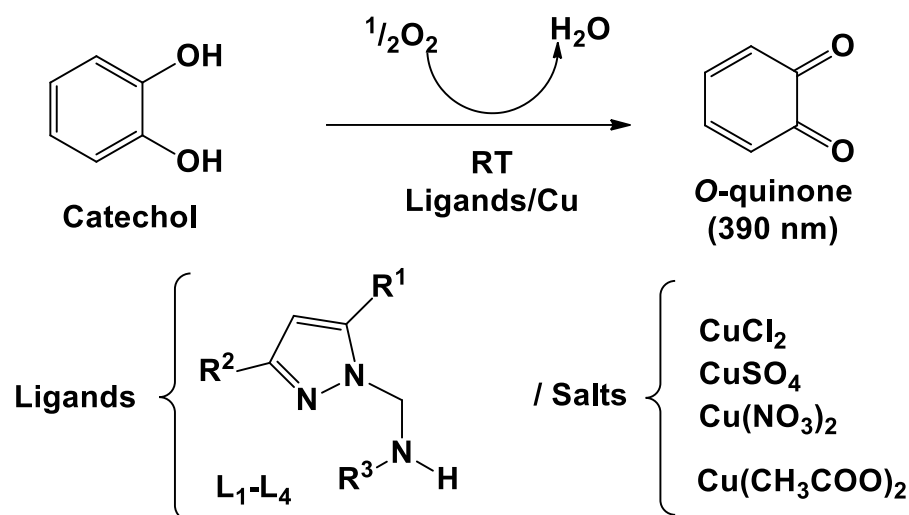


Scheme 1. Synthesis pathway for preparing ligands L₁–L₄.

3. Study of Conversion Reaction of Catechol to *o*-Quinone

The in situ complexes were formed by mixing the organic pyrazole-based ligands with the different copper (II) salts, which were utilized for the oxidation reaction by adding to

the catechol solution under ambient conditions. The oxidation of catechol to *o*-quinone was carried out following the reaction shown in Scheme 2. The oxidation activity was determined directly by recording the absorbance of the *o*-quinones at 390 nm (maximum absorption of *o*-quinone) using UV-Visible absorbance spectroscopy. Firstly, the catechol oxidation reactions were performed without the in situ catalysts in order to validate their effect on the catechol to *o*-quinone conversion reaction under the experimental conditions. It was observed that the absorbance vs. time was almost unchanged, suggesting the role of the in situ catalysts in the oxidation reaction rates.



Scheme 2. General reaction for the oxidation of catechol to *o*-quinone.

3.1. Effect of Concentration

3.1.1. Catalytic Studies Using Ligand/Metal Ratio as 1L/1M in MeOH

The experiments were conducted at room temperature (RT) in methanol (99.99%, MeOH). The complexes were synthesized in situ by successively mixing 0.15 mL of copper (II) salt solution ($2 \times 10^{-3} \text{ mol L}^{-1}$; CuCl_2 , $\text{Cu(CH}_3\text{COO)}_2$, CuSO_4 , and $\text{Cu(NO}_3)_2$) with 0.15 mL of the ligand solution ($2 \times 10^{-3} \text{ mol L}^{-1}$). This step was followed by the addition of 2 mL of a catechol solution (0.1 mol L^{-1}) to the mixture. Finally, the oxidation reaction kinetics was studied by observing the changes in the absorbance of *o*-quinone at 390 nm as a function of time. The results obtained using the ligands (L_1 – L_4) and various copper (II) salts are presented in Figures S16–S19 (see SI).

It is important to study the changes in the absorbance of *o*-quinone when various combinations of the ligands (L_1 – L_4) with the copper (II) salts (CuCl_2 , $\text{Cu(CH}_3\text{COO)}_2$, CuSO_4 , and $\text{Cu(NO}_3)_2$) were used as the catalysts. It was observed that the changes in the absorbance during the oxidation of catechol in the presence of the complex formed by the ligand L_1 and CuSO_4 were greater than those with other copper (II) salts. In the case of L_2 as the ligand with CuCl_2 , very low absorbance was recorded for the oxidation reaction. On the other hand, the absorbance of the *o*-quinone exceeded 1.5 times for all the complexes formed between ligand L_3 and four copper (II) salts, $\text{Cu(NO}_3)_2$, $\text{Cu(CH}_3\text{CO}_2)_2$, CuSO_4 , and CuCl_2 , respectively. While in the case of the complexes formed between ligand L_4 and all four copper (II) salts, the absorbance exceeded 0.8 times (Figure S16). It should be mentioned here that the oxidation rates for the transformation in the presence of in situ complexes formed by the combination of ligands (L_1 – L_4) and copper (II) salts in MeOH in the ratio (1L/1M) are tabulated in Table 1 and calculated by the following expression

$$V = \frac{\Delta A}{\epsilon \cdot L \cdot \Delta t}$$

where A is the absorbance of *o*-quinone measured by UV-vis spectrophotometer at 390 nm, ϵ is the linear molar extinction coefficient expressed in L/mol/cm, L is the optical distance of the cuvette, generally equal to 1 cm, and t is time in min.

Table 1. The reaction rate of catechol oxidation in methanol ($\mu\text{mol L}^{-1} \text{min}^{-1}$) (1L/1M).

L/M	Cu(NO ₃) ₂	Cu(CH ₃ COO) ₂	CuSO ₄	CuCl ₂
L ₁	0.6667	1.9167	3.0104	0.1458
L ₂	12.5521	14.010	14.115	4.1042
L ₃	1.1875	0.5625	4.5833	4.5729
L ₄	0.1562	1.4166	0.7292	1.7083

The results presented in Table 1 revealed that all the copper complexes formed in situ with the ligands L₁–L₄ showed catalytic activity toward the oxidation reaction of catechol to *o*-quinone. However, the oxidation rates differ drastically from 0.1458 $\mu\text{mol L}^{-1} \text{min}^{-1}$ to 14.115 $\mu\text{mol L}^{-1} \text{min}^{-1}$ for the complexes formed between ligand L₁ and CuCl₂ (weak catalyst) and L₂ and CuSO₄ (strong catalyst), respectively.

3.1.2. Catalytic Studies Using Ligand/Metal Ratio as (2L/1M) in Methanol

These complexes were synthesized in situ by successively mixing one equivalent (0.15 mL, $10^{-3} \text{ mol L}^{-1}$) of copper (II) salt solution (CuCl₂, Cu(CH₃COO)₂, CuSO₄, and Cu(NO₃)₂) with two equivalents of a ligand solution (0.15 mL, $2 \times 10^{-3} \text{ mol L}^{-1}$). The resultant mixture was added with 2 mL of catechol solution (0.1 mol L^{-1}). The evolution of absorbance of *o*-quinone at 390 nm with respect to time is shown in Figures 2 and 3, while the oxidation rates are summarized in Table 2.

Table 2. The rate of oxidation of catechol in methanol ($\mu\text{mol}\cdot\text{L}^{-1}\cdot\text{min}^{-1}$) (2L/1M).

2L/1M	Cu(NO ₃) ₂	Cu(CH ₃ COO) ₂	CuSO ₄	CuCl ₂
L ₁	1.1041	—	1.3854	—
L ₂	22.3956	32.2917	16.6563	1.3021
L ₃	6.8333	4.4895	—	—
L ₄	0.4375	1.5104	0.0937	—

As shown in Figure 3, the absorbance of *o*-quinone is more significant when the catechol oxidation reaction was catalyzed by the complexes formed by the ligand L₁ and Cu(NO₃)₂ and CuSO₄, while the other two copper (II) salts led to precipitation, thereby gave the unstable absorbance values. As observed from Figure 1, the absorbance evolution of *o*-quinone was significant when the copper complexes formed by the ligand L₂ and Cu(NO₃)₂, Cu(CH₃COO)₂, and CuSO₄ were used as the catalyst. In contrast, the absorbance remained constant when CuCl₂ was used as the metal salt for the complex formation with ligand L₂. Furthermore, the absorbance value of *o*-quinone for the complex formed by ligand L₃ and Cu(NO₃)₂ and Cu(CH₃COO)₂ was significant, as shown in Figure S21. In contrast, unstable absorbance values were observed in the case of the other two copper salts (CuSO₄ and CuCl₂) due to the precipitation in the reaction. Additionally, the absorbance value for the complex formed by the ligand L₄ with CuSO₄ was greater than those for Cu(CH₃COO)₂ and Cu(NO₃)₂, as shown in Figure S20 (see SI). It was noted that the presence of CuCl₂ led to precipitation in the reaction system, which gave unstable absorbance values. Thus, according to the results summarized in Table 2, it was noted that all copper complexes formed in situ with the ligands L₁–L₄ showed catalytic activity toward the oxidation reaction of catechol to *o*-quinone. However, the oxidation rates differ from 0.0937 $\mu\text{mol L}^{-1} \text{min}^{-1}$ to 32.2917 $\mu\text{mol L}^{-1} \text{min}^{-1}$ for the complexes formed by the ligand L₄ and CuSO₄ (weak catalyst), and L₂ and Cu(CH₃COO)₂ (strong catalyst), respectively.

A comparison of the results presented in Tables 1 and 2 revealed the difference in the oxidation rates of catechol to *o*-quinone. This difference may be related to the effect

of ligand and its concentration which can be explained by the nature of the coordination environment due to the electronic effect of the group. The geometry imposed by the ligand on the metal ion and the characteristics of the steric effect of the ligand may have impacted the coordination and, thus, the activity. Therefore, the effect of the counter anion on the catalytic activity was noted, and the best results were obtained with CH_3COO^- as the anion in the reaction mixture.

3.2. Solvent Effect

To study the effect of the solvent on the rate and efficiency of the catechol oxidation reaction, the experiments were performed under the same reaction conditions with ligand L_2 , using methanol (MeOH), tetrahydrofuran (THF), acetonitrile (CH_3CN), and chloroform (CHCl_3) as the solvents. The oxidation reaction was carried out using the complexes formed in situ by the combinations of two equivalents of ligand L_2 and one equivalent of various copper (II) salts solution in four different solvents. The results summarized in Table 3 showed that a significant change in the absorbance of *o*-quinone was observed when MeOH was used as a solvent to conduct the oxidation reactions using the complexes formed between 2L_2 and $\text{Cu}(\text{NO}_3)_2$ and CuSO_4 . However, the maximum change in the absorbance was recorded when 2L_2 was complexed with $\text{Cu}(\text{CH}_3\text{COO})_2$ in MeOH with the oxidation rate of $32.2917 \mu\text{mol L}^{-1} \text{min}^{-1}$. In contrast, the absorbance showed lower values when THF, CH_3CN , and CHCl_3 were used as the solvents, as shown in Figures S22–S25 (see SI).

Table 3. Catechol oxidation rates for combinations ($2\text{L}/1\text{M}$) in different solvents.

$2\text{L}_2/\text{Copper (II) Salt}$	Solvents	$V (\mu\text{mol}\cdot\text{L}^{-1}\cdot\text{min}^{-1})$
$2\text{L}_2/\text{Cu}(\text{NO}_3)_2$	MeOH	22.3958
	THF	1.1667
	CH_3CN	0.0417
	CHCl_3	0.3021
$2\text{L}_2/\text{Cu}(\text{CH}_3\text{COO})_2$	MeOH	32.2917
	THF	5.5625
	CH_3CN	0.0417
	CHCl_3	0.1458
$2\text{L}_2/\text{CuSO}_4$	MeOH	16.6563
	CH_3CN	0.1458
	CHCl_3	0.2604
$2\text{L}_2/\text{CuCl}_2$	MeOH	0.1302
	THF	0.1812
	CH_3CN	0.0021
	CHCl_3	0.0208

The above-mentioned results indicated the notable effect of solvent on the catalytic activity of the in situ catalysts. Methanol, a polar protic solvent, was considered the best solvent among all, as better catalytic activity was shown by the complexes in this solvent. Moreover, it showed improved results when compared to THF, which is a polar aprotic solvent. Assuming that the general physical parameters of the solvents, including dielectric constant, dipole moment, and polarity, have no significant effect on the activity of the complexes in oxidizing catechol, as a consequence, it can be hypothesized that the coordination power or the protic nature of the solvents are the most important factors that can alter the catalytic activity of the system [39–41]. It has been widely reported that polar protic solvents can strongly solvate X anions ($\text{X} = \text{Cl}^-$, CH_3COO^- , SO_4^{2-} , and NO_3^-) by forming hydrogen bonding with them. Hence, the hydrogen bonding keeps the anions isolated, resulting in the least reactivity in this solvent system, whereas the counterion also solvated the cationic copper ions. However, due to the absence of hydrogen bonding in the case of cations, the solvation is comparatively less strong, leaving the cations to be more reactive. This reactivity, in turn, facilitated the formation of the complexes between the

ligands and cations, which overall increased the rate of oxidation of catechol to *o*-quinone. To validate the effect of solvent on the catalytic activity, the ligand combination (2L/1M) was tested using $2L_2/Cu(CH_3COO)_2$, $2L_2/Cu(NO_3)_2$, and $2L_2/CuSO_4$ in MeOH. The kinetic experiments were performed at room temperature, and the absorbance evolution of *o*-quinone was recorded every 5 min, as shown in Figures 1–3. The appearance of an intense band at 390 nm for the three combinations, $2L_2/Cu(CH_3COO)_2$, $2L_2Cu(NO_3)_2$, and $2L_2CuSO_4$ in MeOH confirmed that the catechol could be successfully oxidized to *o*-quinone with these combinations of catalysts.

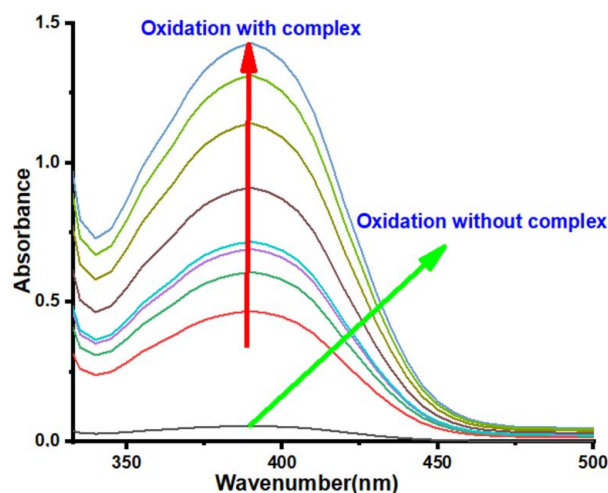


Figure 1. Absorbance spectrum of *o*-quinone as a function of time for the $2L_2/CuSO_4$ combination.

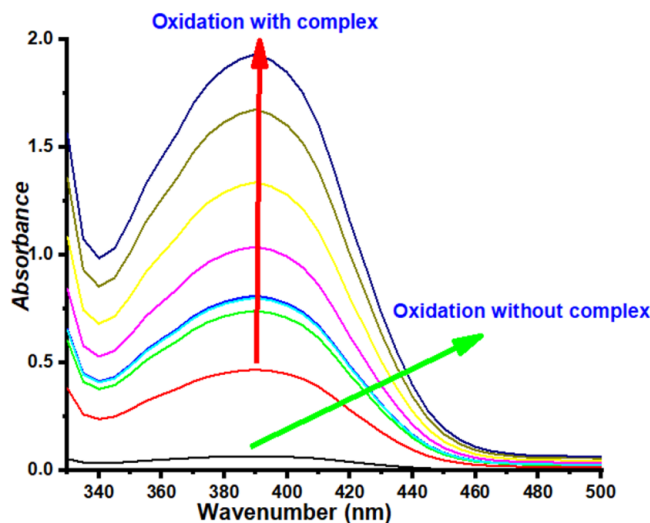


Figure 2. Absorbance spectrum of *o*-quinone as a function of time for the combination $L_2/Cu(CH_3COO)_2$.

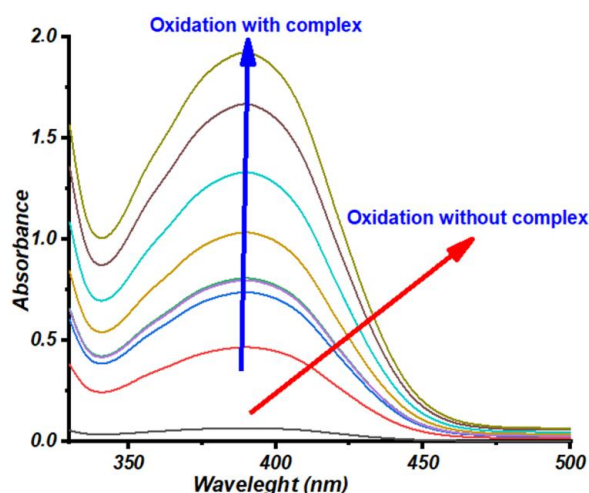


Figure 3. Absorbance spectrum of *o*-quinone as a function of time for the combination $2L_2/Cu(NO_3)_2$.

3.3. Kinetic Study

The kinetics of the oxidation reaction was studied to get more information on the catalytic efficiency of the complexes. This study was conducted to determine the kinetics parameters, such as V_{max} (maximum reaction rate) and K_m (reaction constant), using the initial rate method. The experiments were conducted in MeOH using the ligand-metal combinations as $2L_2/Cu(NO_3)_2$, $2L_2/Cu(CH_3COO)_2$, and $2L_2/CuSO_4$ under ambient conditions. This was treated with various concentrations of catechol substrate ranging from $4 \times 10^{-2} \text{ mol L}^{-1}$ to $4 \times 10^{-1} \text{ mol L}^{-1}$. The evolution of the absorbance of *o*-quinone at 390 nm was observed and recorded as a function of time, and then the relationship between initial rates, V_i ($\mu\text{mol L}^{-1} \text{ min}^{-1}$), and the substrate (catechol) concentration was established (mol L^{-1}).

As shown in Figures S26–S28 (see SI), a linear relationship between the initial velocities and substrate concentration was obtained; thus, the Michaelis–Menten model was applied to obtain the kinetic parameters in the reaction, summarized in Table 4. The results showed that the reactions rates, V_{max} , varied from $41.67 \mu\text{mol L}^{-1} \text{ min}^{-1}$ to $33.56 \mu\text{mol L}^{-1} \text{ min}^{-1}$ to $32.86 \mu\text{mol L}^{-1} \text{ min}^{-1}$ when the combination $2L_2/Cu(CH_3COO)_2$, $2L_2/CuSO_4$, and $2L_2/Cu(NO_3)_2$ was used for the catalysis, respectively. Furthermore, a low value of K_m was obtained for the combination $2L_2/Cu(CH_3COO)_2$, demonstrating that MeOH is the suitable solvent for this catalytic study. It should be mentioned here that the smaller value of K_m results in the greater affinity of the catalyst toward the catechol substrate [42]. Thus, the best results were obtained in the case of $2L_2/Cu(CH_3COO)_2$, which achieved the highest catalytic efficiency.

Table 4. Values of the V_{max} and K_m constants.

$2L_2/Cu(II)$ Salt	V_{max} ($\mu\text{mol} \cdot \text{L}^{-1} \cdot \text{min}^{-1}$)	K_m ($\text{mol} \cdot \text{L}^{-1}$)
$2L_2/Cu(NO_3)_2$	32.86	0.04
$2L_2/Cu(CH_3COO)_2$	41.67	0.02
$2L_2/CuSO_4$	33.56	0.06

4. Conclusions

In summary, the catalytic activity of complexes formed by pyrazole-based ligands and different copper (II) salts were studied for the oxidation reaction of catechol. It was found that all combinations could catalyze the oxidation of catechol to *o*-quinone; however, their reaction rates varied under ambient conditions in the presence of atmospheric oxygen as the oxidant. It was also demonstrated that the reaction rates and catalytic efficiency of the particular combination were influenced by the nature and concentration of ligands with the combination (2L/1M) as an excellent catalyst. In addition, the nature of the

solvent significantly affected the catalytic activity of the in situ complexes. Furthermore, the combinations of $\text{Cu}(\text{CH}_3\text{COO})_2$ with the pyrazole-based ligands in methanol were found to be more effective in catalyzing the oxidation reaction, suggesting the significant role of the counterion on the activity. The kinetics of the oxidation reaction was also studied using the Michaelis–Menten model and demonstrated that the results were in agreement with this model. It was reported that the combinations $2\text{L}_2/\text{Cu}(\text{CH}_3\text{COO})_2$, $2\text{L}_2/\text{CuSO}_4$, and $2\text{L}_2/\text{Cu}(\text{NO}_3)_2$ in MeOH were considered the best catalysts for the oxidation reaction of catechol.

Supplementary Materials: The following supporting information can be downloaded at: <https://www.mdpi.com/article/10.3390/catal13010162/s1>, Figure S1: ^1H NMR spectrum of L_1 in DMSO (400 MHz); Figure S2: ^{13}C NMR spectrum of L_1 in DMSO (400 MHz); Figure S3: FT-IR spectrum of L_1 ; Figure S4: ^1H NMR spectrum of L_2 in DMSO (400 MHz); Figure S5: ^{13}C NMR spectrum of L_2 in DMSO (400 MHz); Figure S6: DEPT-135 NMR spectrum of L_2 in DMSO (400 MHz); Figure S7: FT-IR spectrum of L_2 ; Figure S8: ^1H NMR spectrum of L_3 in DMSO (400 MHz); Figure S9: ^{13}C NMR spectrum of L_3 in DMSO (400 MHz); Figure S10: DEPT-135 NMR spectrum of L_3 in DMSO (400 MHz); Figure S11: FT-IR spectrum of L_3 ; Figure S12: ^1H NMR spectrum of L_4 in DMSO (400 MHz); Figure S13: ^{13}C NMR spectrum of L_4 in DMSO (400 MHz); Figure S14: ^{13}C NMR spectrum of L_4 in DMSO (400 MHz); Figure S15: FT-IR spectrum of L_4 ; Figure S16: Absorbance evolution of *o*-quinone in presence of complexes formed by L_1 and different copper salts in MeOH; Figure S17: Absorbance evolution of *o*-quinone in presence of complexes formed by L_2 and different copper salts in MeOH; Figure S18: Absorbance evolution of *o*-quinone in presence of complexes formed by L_3 and different copper salts in MeOH; Figure S19: Absorbance evolution of *o*-quinone in presence of complexes formed by L_4 and different copper salts in MeOH; Figure S20: Absorbance evolution of *o*-quinone in presence of complexes formed by L_1 and L_4 with different copper salts in MeOH; Figure S21: Absorbance evolution of *o*-quinone in presence of complexes formed by L_2 and L_3 with different copper salts in MeOH; Figure S22: Absorbance evolution of *o*-quinone in presence of complexes formed by $2\text{L}_2/\text{Cu}(\text{NO}_3)_2$ in different solvents; Figure S23: Absorbance evolution of *o*-quinone in presence of complexes formed by $2\text{L}_2/\text{Cu}(\text{CH}_3\text{COO})_2$ in different solvents; Figure S24: Absorbance evolution of *o*-quinone in presence of complexes formed by $2\text{L}_2/\text{CuCuSO}_4$ in different solvents; Figure S25: Absorbance evolution of *o*-quinone in presence of complexes formed by $2\text{L}_2/\text{CuCl}_2$ in different solvents; Figure S26: Reaction dependence on the concentration of catechol using $2\text{L}_2/\text{Cu}(\text{NO}_3)_2$; Figure S27: Reaction dependence on the concentration of catechol using $2\text{L}_2/\text{Cu}(\text{CH}_3\text{COO})_2$; Figure S28: Reaction dependence on the concentration of catechol using $2\text{L}_2/\text{CuSO}_4$.

Author Contributions: Conceptualization, R.T. and B.H.; methodology, K.Z. and A.T.; software, A.T.; validation, B.H. and K.Z.; formal analysis, E.B.Y. and M.E.K.; investigation, R.T.; data curation, A.T. and K.Z.; writing—original draft preparation, A.T., K.Z. and M.E.K.; writing—review and editing, A.Y.A.A. and A.M.; supervision, R.T., M.E.K. and E.B.Y.; project administration, A.Y.A.A. and A.M.; funding acquisition, supervision & validation; A.Y.A.A. and M.A. All authors have read and agreed to the published version of the manuscript.

Funding: King Khalid University, project number RGP.2/226/43.

Data Availability Statement: Please feel free to contact the authors.

Acknowledgments: The authors extend their appreciation to the Deanship of Scientific Research at King Khalid University for funding this work through Large Groups Project under grant number RGP.2/226/43.

Conflicts of Interest: The authors declare no conflict of interest.

References

1. Bouroumane, N.; El Kodadi, M.; Touzani, R.; El Boutaybi, M.; Oussaid, A.; Hammouti, B.; Nandiyanto, A.B.D. New Pyrazole-Based Ligands: Synthesis, Characterization, and Catalytic Activity of Their Copper Complexes. *Arab. J. Sci. Eng.* **2022**, *47*, 269–279. [[CrossRef](#)]
2. Titi, A.; Almutairi, S.M.; Touzani, R.; Messali, M.; Tillard, M.; Hammouti, B.; El Kodadi, M.; Eddike, D.; Zarrouk, A.; Warad, I. A new mixed pyrazole-diamine/Ni(II) complex, Crystal structure, physicochemical, thermal and antibacterial investigation. *J. Mol. Struct.* **2021**, *1236*, 130304. [[CrossRef](#)]
3. Kaddouri, Y.; Abridgach, F.; Ouahhoud, S.; Benabbes, R.; El Kodadi, M.; Alsalme, A.; Al-Zaqri, N.; Warad, I.; Touzani, R. Synthesis, characterization, reaction mechanism prediction and biological study of mono, bis and tetrakis pyrazole derivatives against *Fusarium oxysporum* f. sp. *Albedinis* with conceptual DFT and ligand-protein docking studies. *Bioorg. Chem.* **2021**, *110*, 104696. [[CrossRef](#)]
4. Ouadi, Y.E.; Lamsayah, M.; Bendaif, H.; Benhiba, F.; Touzani, R.; Warad, I.; Zarrouk, A. Electrochemical and theoretical considerations for interfacial adsorption of novel long chain acid pyrazole for mild steel conservation in 1 M HCl medium. *Chem. Data Collec.* **2021**, *31*, 100638. [[CrossRef](#)]
5. Kaddouri, Y.; Bouchal, B.; Abridgach, F.; El Kodadi, M.; Bellaoui, M.; Touzani, R. Synthesis, Molecular Docking, MEP and SAR Analysis, ADME-Tox Predictions, and Antimicrobial Evaluation of Novel Mono-and Tetra-Alkylated Pyrazole and Triazole Ligands. *J. Chem.* **2021**, *2021*, 6663245. [[CrossRef](#)]
6. Titi, A.; Messali, M.; Alqurashy, B.A.; Touzani, R.; Shiga, T.; Oshio, H.; Fettouhi, M.; Rajabi, M.; Almalki, F.A.; Ben Hadda, T. Synthesis, characterization, X-Ray crystal study and bioactivities of pyrazole derivatives: Identification of antitumor, antifungal and antibacterial pharmacophore sites. *J. Mol. Struct.* **2020**, *1205*, 127625. [[CrossRef](#)]
7. Kaddouri, Y.; Abridgach, F.; Yousfi, E.B.; El Kodadi, M.; Touzani, R. New thiazole, pyridine and pyrazole derivatives as antioxidant candidates: Synthesis, DFT calculations and molecular docking study. *Heliyon* **2020**, *6*, e03185. [[CrossRef](#)]
8. Khoutoul, M.; Djedouani, A.; Lamsayah, M.; Abridgach, F.; Touzani, R. Liquid-liquid extraction of metal ions, DFT and TD-DFT analysis for some pyrane derivatives with high selectivity for Fe(II) and Pb(II). *Sep. Sci. Technol.* **2016**, *51*, 1112–1123. [[CrossRef](#)]
9. Abridgach, F.; Bouchal, B.; Riant, O.; Macé, Y.; Takfaoui, A.; Radi, S.; Oussaid, A.; Bellaoui, M.; Touzani, R. New N,N,N',N'-tetradentate pyrazoly agents: Synthesis and evaluation of their antifungal and antibacterial activities. *Med. Chem.* **2016**, *12*, 83–89. [[CrossRef](#)]
10. Takfaoui, A.; Zhao, L.; Touzani, R.; Dixneuf, P.H.; Doucet, H. Palladium-catalysed direct diarylations of pyrazoles with aryl bromides: A one step access to 4,5-diarylpzrazoles. *Tetrahedron Lett.* **2015**, *55*, 1697–1701. [[CrossRef](#)]
11. Penning, T.D.; Talley, J.J.; Bertenshaw, S.R.; Carter, J.S.; Collins, P.W.; Docter, S.; Graneto, M.J.; Lee, L.F.; Miyashiro, J.M.; Rogers, R.S.; et al. Synthesis and biological evaluation of the 1,5-diarylpzrazole class of cyclooxygenase-2 inhibitors: Identification of 4-[5-(4-methylphenyl)-3(trifluoromethyl)-1h-pyrazol-1-yl]benzenesulfonamide (sc-58635, celecoxib). *J. Med. Chem.* **1997**, *40*, 1347–1365. [[CrossRef](#)]
12. Lv, P.-C.; Li, H.-Q.; Sun, J.; Zhou, Y.; Zhu, H.-L. Synthesis and biological evaluation of pyrazole derivatives containing thiourea skeleton as anticancer agents. *Bioorg. Med. Chem.* **2010**, *18*, 4606–4614. [[CrossRef](#)]
13. Faria, J.V.; Vegi, P.F.; Miguita, A.G.C.; dos Santos, M.S.; Boechat, N.; Bernardino, A.M.R. Recently reported biological activities of pyrazole compounds. *Bioorg. Med. Chem.* **2017**, *25*, 5891–5903. [[CrossRef](#)]
14. Zavozin, A.G.; Ignat'ev, N.V.; Schulte, M.; Zlotin, S.G. Synthesis of novel tridentate pyrazole–bipyridine ligands for Co-complexes as redox-couples in dye-sensitized solar cells. *Tetrahedron* **2015**, *71*, 8551–8556. [[CrossRef](#)]
15. Megyes, T.; May, Z.; Schubert, G.; Grósz, T.; Simándi, L.I.; Radnai, T. Synthesis and structure study of some catecholase-mimetic iron complexes. *Inorg. Chim. Acta* **2006**, *359*, 2329–2336. [[CrossRef](#)]
16. Ayad, M.I. Synthesis, characterization and catechol oxidase biomimetic catalytic activity of cobalt (II) and copper (II) complexes containing N2O2 donor sets of imine ligands. *Arab. J. Chem.* **2016**, *9*, S1297–S1306. [[CrossRef](#)]
17. Dey, S.K.; Mukherjee, A. The synthesis, characterization and catecholase activity of dinuclear cobalt (II/III) complexes of an O-donor rich Schiff base ligand. *New J. Chem.* **2014**, *38*, 4985–4995. [[CrossRef](#)]
18. Saddik, R.; Abridgach, F.; Benchat, N.; El Kadiri, S.; Hammouti, B.; Touzani, R. Catecholase activity; investigation for pyridazinone- and thiopyridazinone-based ligands. *Res. Chem. Inter.* **2012**, *38*, 1987–1998. [[CrossRef](#)]
19. Mouadili, A.; Attayibat, A.; El Kadiri, S.; Radi, S.; Touzani, R. Catecholase activity investigations using in situ copper complexes with pyrazole and pyridine based ligands. *Appl. Cat. A Gen.* **2013**, *454*, 93–99. [[CrossRef](#)]
20. Marion, R.; Saleh, N.M.; Le Poul, N.; Lavastre, D.; Geneste, F. Rate enhancement of the catechol oxidase activity of a series of biomimetic monocopper (II) complexes by introduction of non-coordinating groups in N-tripodal ligands. *New J. Chem.* **2012**, *36*, 1828–1835. [[CrossRef](#)]
21. Sarkar, S.; Sim, A.; Kim, S.; Lee, H.I. Catecholase activity of a self-assembling dimeric Cu (II) complex with distant Cu (II) centers. *J. Mol. Cat. A Chem.* **2015**, *410*, 149–159. [[CrossRef](#)]
22. Allam, A.; Dechamps-Olivier, I.; Behr, J.B.; Dupont, L.; Plantier-Royon, R. Thermodynamic, spectroscopic studies and catechol oxidase activity of copper (II) complexes with amphiphilic d-galacturonic acid derived ligands. *Inorg. Chim. Acta* **2011**, *366*, 310–319. [[CrossRef](#)]
23. Titi, A.; Al-Noaimi, M.; Kaddouri, Y.; El Ati, R.; Yousfi, E.B.; El Kodadi, M.; Touzani, R. Study of the catecholase catalytic properties of copper (II) complexes prepared in-situ with monodentate ligands. *Mater. Today Proc.* **2019**, *13*, 1134–1142. [[CrossRef](#)]

24. El Boutaybi, M.; Titi, A.; Alzahrani, A.Y.A.; Bahari, Z.; Tillard, M.; Hammouti, B.; Touzani, R. Aerial Oxidation of Phenol/Catechol in the Presence of Catalytic Amounts of $[(Cl)_2Mn(RCOOET)]$, $RCOOET=Ethyl-5-Methyl-1-((6-methyl-3-nitropyridin-2-yl)amino)methyl)-1Hpyrazole-3-carboxylate$. *Catalysts* **2022**, *12*, 1642. [[CrossRef](#)]
25. Titi, A.; Rachid Touzani, R.; Moliterni, A.; Giacobbe, C.; Baldassarre, F.; Taleb, M.; Al-Zaqri, N.; Zarrouk, A.; Warad, I. Ultrasonic Clusterization Process to Prepare $[(NNCO)_6Co_4Cl_2]$ as a Novel Double-Open- Co_4O_6 Cubane Cluster: SXR D Interactions, DFT, Physicochemical, Thermal Behaviors, and Biomimicking of Catecholase Activity. *ACS Omega* **2022**, *7*, 32949. [[CrossRef](#)]
26. Titi, A.; Shiga, T.; Oshio, H.; Touzani, R. Synthesis of novel $Cl_2Co_4L_6$ cluster using 1-hydroxymethyl-3, 5-dimethylpyrazole (LH) ligand: Crystal structure, spectral, thermal, Hirschfeld surface analysis and catalytic oxidation evaluation. *J. Mol. Struct.* **2020**, *1199*, 126995. [[CrossRef](#)]
27. Titi, A.; Warad, I.; Tillard, M.; Messali, M.; Touzani, R. Inermolecular interaction in $[C_6H_{10}N_3]_2[CoCl_4]$ complex: Synthesis, XRD/HSA relation, spectral and catecholase catalytic analysis. *J. Mol. Struct.* **2020**, *1217*, 128422. [[CrossRef](#)]
28. Titi, A.; Oshio, H.; Messali, M.; Touzani, R.; Warad, I. Synthesis and XRD of Novel Ni 4 (μ_3-O)₄ Twist Cubane Cluster Using Three NNO Mixed Ligands: Hirshfeld, Spectral, Thermal and Oxidation Properties. *J. Cluster Sci.* **2020**, *32*, 227–234. [[CrossRef](#)]
29. El Kodadi, M.; Malek, F.; Touzani, R.; Ramdani, A. Synthesis of new tripodal ligand 5-(bis (3, 5-dimethyl-1H-pyrazol-1-ylmethyl) amino) pentan-1-ol, catecholase activities studies of three functional tripodal pyrazolyl N-donor ligands, with different copper (II) salts. *Cat. Commun.* **2008**, *9*, 966–969. [[CrossRef](#)]
30. Elmsellem, H.; Harit, T.; Aouniti, A.; Malek, F.; Riahi, A.; Chetouani, A.; Hammouti, B. Adsorption properties and inhibition of mild steel corrosion in 1 M HCl solution by some bipyrazolic derivatives: Experimental and theoretical investigations. *Prot. Met. Phys. Chem. Sur.* **2015**, *51*, 873–884. [[CrossRef](#)]
31. Touzani, R.; Ramdani, A.; Ben-Hadda, T.; El Kadiri, S.; Maury, O.; Le Bozec, H.; Dixneuf, P.H. Efficient synthesis of new nitrogen donor containing tripods under microwave irradiation and without solvent. *Synth. Commun.* **2001**, *31*, 1315–1321. [[CrossRef](#)]
32. Bouabdallah, I.; Touzani, R.; Zidane, I.; Ramdani, A. Synthesis of new tripodal ligand: N,N-bis [(1, 5-dimethylpyrazol-3-yl) methyl] benzylamine.: Catecholase activity of two series of tripodal ligands with some copper (II) salts. *Catal. Commun.* **2007**, *8*, 707–712. [[CrossRef](#)]
33. Harit, T.; Malek, F.; El Bali, B.; Khan, A.; Dalvandi, K.; Marasini, B.P.; Noreen, S.; Malik, R.; Khan, S.; Choudhary, M.I. Synthesis and enzyme inhibitory activities of some new pyrazole-based heterocyclic compounds. *Med. Chem. Res.* **2012**, *21*, 2772–2778. [[CrossRef](#)]
34. El Kodadi, M.; Benamar, M.; Bouabdallah, I.; Zyad, A.; Malek, F.; Touzani, R.; Ramdani, A.; Melhaoui, A. New synthesis of two tridentate bipyrazolic compounds and their cytotoxic activity tumor cell lines. *Nat. Prod. Res.* **2007**, *21*, 947–952. [[CrossRef](#)]
35. Kaddouri, Y.; Haddari, H.; Titi, A.; Yousfi, E.B.; Chetouani, A.; Touzani, R. Catecholase catalytic properties of copper (II) complexes prepared in-situ with heterocyclic ligands: Experimental and DFT study. *Mor. J. Chem.* **2020**, *8*, 8-1.
36. Harit, T.; Isaad, J.; Malek, F. Novel efficient functionalized tetrapyrazolic macrocycle for the selective extraction of lithium cations. *Tetrahedron* **2016**, *72*, 2227–2232. [[CrossRef](#)]
37. Ding, H.Y.; Cheng, H.J.; Wang, F.; Liu, D.X.; Li, H.X.; Fang, Y.Y.; Zhao, W.; Lang, J.P. [(bmpppy) Cu (μ -I)]₂ (bmpppy = 2,6-bis (1-methyl-1H-pyrazol-3-yl) pyridine): Synthesis, crystal structure and its catalytic performance for MMA polymerization. *J. Organomet. Chem.* **2013**, *741*, 1–6. [[CrossRef](#)]
38. Titi, A.; Touzani, R.; Moliterni, A.; Ben Hadda, T.; Messali, M.; Benabbes, R.; Berredjem, M.; Bouzina, A.; Al-Zaqri, N.; Taleb, M.; et al. Synthesis, Structural, Biocomputational Modeling and Antifungal Activity of Novel Armed pyrazoles. *J. Mol. Struct.* **2022**, *1264*, 133156. [[CrossRef](#)]
39. Zerrouki, A.; Touzani, R.; Bouabdallah, I.; El Kadiri, S.; Ghalem, S. Synthesis of new derivatized pyrazole based ligands and their catecholase activity studies. *Arab. J. Chem.* **2011**, *4*, 459–464. [[CrossRef](#)]
40. Banu, K.S.; Mukherjee, M.; Guha, A.; Bhattacharya, S.; Zangrando, E.; Das, D. Dinuclear copper(2) complexes:solvent dependent catecholase activity. *Polyhedron* **2012**, *45*, 245–254. [[CrossRef](#)]
41. Boussalah, N.; Touzani, R.; Bouabdallah, I.; Ghalem, S.; El Kadiri, S. Oxidation catalytic properties of new amino acid based on pyrazole tripodal ligands. *Inter. J. Acad. Res.* **2009**, *1*, 137–143.
42. Takfaoui, A.; Lamsayah, M.; El Ouafi, A.; Oussaid, A.; Kabouche, Z.; Touzani, R. N,N'-bipyrazole compounds: Effect of concentration, solvent, ligand and metal anions on the catecholase properties. *J. Mater. Environ. Sci.* **2015**, *6*, 2129–2136.

Disclaimer/Publisher's Note: The statements, opinions and data contained in all publications are solely those of the individual author(s) and contributor(s) and not of MDPI and/or the editor(s). MDPI and/or the editor(s) disclaim responsibility for any injury to people or property resulting from any ideas, methods, instructions or products referred to in the content.